



Title	Polyether/Polythioether Synthesis via Ring-Opening Polymerization of Epoxides and Episulfides Catalyzed by Alkali Metal Carboxylates
Author(s)	Gao, Tianle; Xia, Xiaochao; Tajima, Kenji et al.
Citation	Macromolecules, 55(21), 9373-9383 <a href="https://doi.org/10.1021/acs.macromol.2c00656">https://doi.org/10.1021/acs.macromol.2c00656</a>
Issue Date	2022-10-21
Doc URL	<a href="https://hdl.handle.net/2115/90596">https://hdl.handle.net/2115/90596</a>
Rights	This document is the Accepted Manuscript version of a Published Work that appeared in final form in Macromolecules, copyright © American Chemical Society after peer review and technical editing by the publisher. To access the final edited and published work see <a href="https://pubs.acs.org/articlesonrequest/AOR-BTR4QWR958AZSCX33UMA">https://pubs.acs.org/articlesonrequest/AOR-BTR4QWR958AZSCX33UMA</a> .
Type	journal article
File Information	Manuscript.pdf



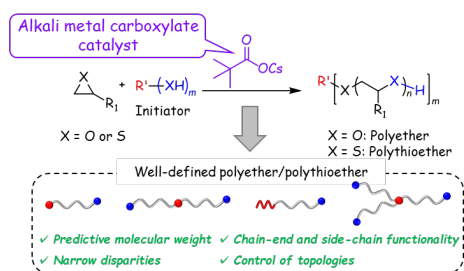
# Polyether/Polythioether Synthesis via Ring-Opening Polymerization of Epoxides and Episulfides Catalyzed by Alkali Metal Carboxylates

Tianle Gao,<sup>#</sup> Xiaochao Xia,<sup>#,§</sup> Kenji Tajima,<sup>^</sup> Takuya Yamamoto,<sup>^</sup> Takuya Isono,<sup>\*,^</sup> Toshifumi Satoh<sup>\*,^</sup>

<sup>#</sup>Graduate School of Chemical Sciences and Engineering, Hokkaido University, Sapporo 060-8628, Japan

<sup>^</sup>Division of Applied Chemistry, Faculty of Engineering, Hokkaido University, Sapporo 060-8628, Japan

<sup>§</sup>School of Materials Science and Engineering, Chongqing University of Technology, Chongqing 400054, China



For Table of Contents use only

ABSTRACT. Alkali metal carboxylates were evaluated as simple and green catalysts for the ring-opening polymerization (ROP) of various epoxides (e.g., alkyl-substituted epoxides and glycidyl ethers) and episulfides (alkyl-substituted episulfides and thioglycidyl ethers). The thus produced functional polyethers (end-functionalized polyethers, block copolyethers, polyether-polyester block copolymers, topologically unique polyethers, and isotactic-enriched polyethers) and polythioethers featured well-defined structures and controlled molecular weights ( $M_{n,SEC} = 1.0\text{--}32$  kg mol<sup>-1</sup>). The most effective catalyst was identified as cesium pivalate, and the variation of carboxylate moieties and alkali metal cations enabled the tuning of acid/base characteristics and thus allowed one to control polymerization behavior and expand the scope of functional monomers and initiators. Kinetic analysis confirmed the controlled/living nature of the polymerization process, while mechanistic studies revealed that carboxylate moieties did not directly initiate the ring-opening of epoxide monomers via nucleophilic attack but rather activated the alcohol initiators/chain ends via H-bonding and thus rendered the corresponding OH groups sufficiently nucleophilic to attack the alkali metal cation-activated epoxides.

## INTRODUCTION

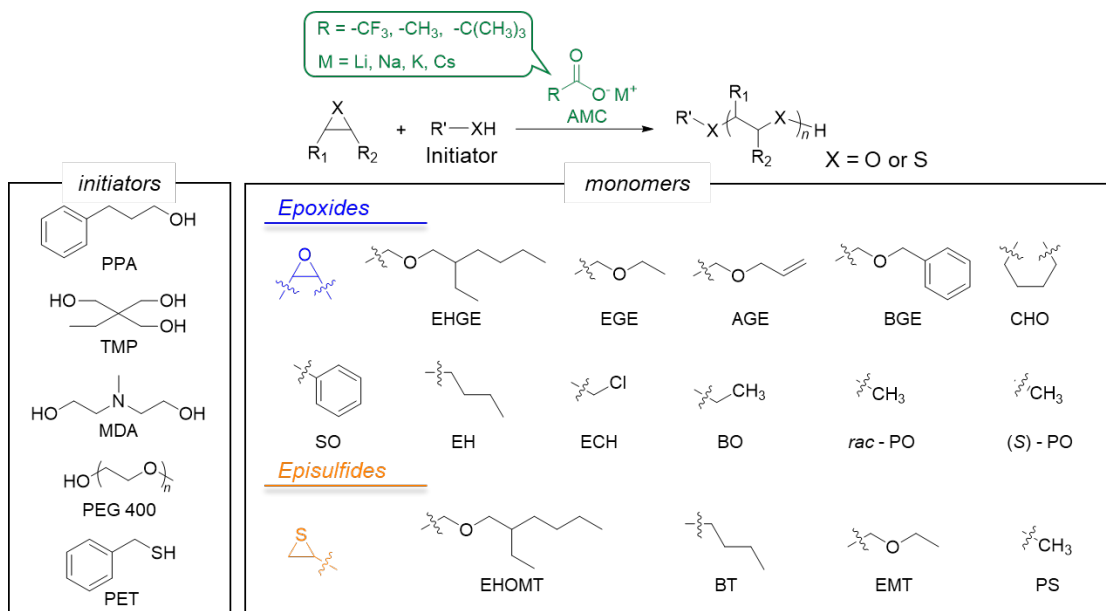
Polyethers, which are typically synthesized via the ROP of epoxides, are an important class of polymers with numerous applications such as antifouling coatings,<sup>1</sup> cosmetics,<sup>2</sup> biomedical materials,<sup>3,4,5</sup> and rubber/plastics.<sup>6,7</sup> Some of the most common polyethers, poly(ethylene glycol) and poly(propylene glycol), are obtained from the readily available ethylene oxide and propylene oxide (PO), respectively, and are used as low-molecular-weight hydroxyl-terminated chains for polyurethane manufacturing.<sup>6</sup> Moreover, poly(ethylene glycol) is employed as the gold standard

biocompatible polymer to modify biomolecules such as proteins, peptides, and non-peptides and thus endow them with “stealth properties” such as prolonged blood circulation, increased stability against degradation by metabolic enzymes, and reduced or eliminated immunoresponses.<sup>8</sup>

Conventionally, polyethers are mainly synthesized by anionic ROP initiated by sodium, potassium, or cesium alkoxides.<sup>9,10</sup> In this system, the countercation plays a key role and should exhibit low Lewis acidity and little or no interaction with the oxyanionic end of the growing chain, thus allowing the oxyanion to efficiently act as a nucleophile and engage in chain growth. However, at high temperatures, the strong basicity of alkali metal alkoxides gives rise to irreversible chain transfer to the monomer with methylene- or methyl-group substituent, which affords an unwanted  $\alpha$ -chain end and seriously limits the accessible molecular weight of the product ( $\leq 5.0 \text{ kg mol}^{-1}$ ). Therefore, new catalytic systems for the optimization of epoxide ROP are highly sought after. The most representative case is the addition of crown ethers to alkali metal alkoxide systems,<sup>11,12</sup> which accelerates polymerization and effectively suppresses chain transfer, thereby allowing the synthesis of polyethers with high number-averaged molecular weights ( $M_n > 10 \text{ kg mol}^{-1}$ ) and low dispersities ( $D_M \approx 1.2$ ). Another example is the alkali metal alkoxide/trialkylaluminum system,<sup>13,14,15,16</sup> in which the monomer is effectively activated and becomes more susceptible to ring-opening. Although metal complex catalysts facilitate the synthesis of stereoregular polyethers even from racemic epoxide monomers,<sup>17,18,19</sup> the biomedical and environmental applications of these catalysts are limited by the problematic and time-consuming removal of toxic metals (e.g., Co and Cr) from the related catalyst residues. The need for heavy-metal-free and eco-friendly ROP systems following the green chemistry concept has inspired the development of various organocatalysts allowing the ROP of epoxides to proceed in a highly efficient and controllable manner under mild conditions. However, these organocatalysts exhibit several drawbacks, e.g.,

highly reactive and sensitive catalysts such as *N*-heterocyclic carbenes and *N*-heterocyclic olefins require careful handling to avoid the adverse effects of moisture and temperature variation.<sup>20,21</sup> In the case of the phosphazene base (*t*-Bu-P<sub>4</sub>) catalyst system, the deprotonation of protic functional groups limits the scope of epoxide monomers, and the catalyst residues are suspected to be cytotoxic.<sup>22</sup> Besides, the high cost (compared to that of conventional alkoxides) of organocatalysts obstructs their application in industrial polyether production.

Our group has recently reported an efficient and simple alkali metal carboxylate (AMC) catalyst for the ROP of cyclic esters and the one-step synthesis of sequence-controlled multiblock copolymers.<sup>23,24,25,26</sup> Notably, AMC basicity can be tuned through the variation of carboxylate moieties and counteranions to achieve controlled/living polymerization. AMCs are well suited for industrial use in view of their low cost, ease of handling, and low toxicity, and can also initiate the ring-opening alternating copolymerization (ROAC) of epoxides and cyclic anhydrides.<sup>26</sup> During ROAC, epoxides act as polar solvents to weaken the coulombic interaction between the metal cation (Lewis acid) and the carboxylate anion (Lewis base). Coordination with metal cations activates epoxides toward nucleophilic attack, while carboxylates are sufficiently reactive to attack the activated epoxides and induce their ring-opening, e.g., potassium carboxylates can initiate the anionic ROP of epoxides in the presence of a crown ether.<sup>27</sup> However, our previous studies suggest that the role of AMCs can change from initiator to catalyst in the co-presence of an alcohol initiator. Herein, we developed a new epoxide ROP system with AMCs as catalysts for the synthesis of polyethers, showed that this system offers the benefits of excellent molecular weight controllability with low dispersity ( $D_M$ ) and a broad substrate/initiator scope compared to reported alkali metal alkoxide-initiated system,<sup>9,11,13</sup> and used it to synthesize well-defined polythioethers via the ROP of episulfides (Scheme 1).



**Scheme 1.** Ring-opening polymerization of epoxides and episulfides catalyzed by alkali metal carboxylates.

## MATERIALS

**Materials.** 2-Ethylhexyl glycidyl ether (EHGE; >98.0%, Tokyo Kasei Kogyo Co., Ltd. (TCI)), ethyl glycidyl ether (EGE; >98.0%, TCI), allyl glycidyl ether (AGE; >99.0%, TCI), benzyl glycidyl ether (BGE; >97.0%, TCI), styrene oxide (SO; >98.0%, TCI), 1,2-epoxyhexane (EH; >96.0%, TCI), 1,2-epoxycyclohexane (CHO; >98.0%, TCI), epichlorohydrin (ECH; >99.0%, TCI), 1,2-butylene oxide (BO; >99.0%, TCI), 3-phenyl-1-propanol (PPA; >98.0%, TCI), *N*-methyldiethanolamine (MDA; >99.0%, TCI), 2-phenylethanethiol (PET; >97.0%, TCI), and tributylphosphine (TBP; >95.0%, TCI) were purified by distillation with CaH<sub>2</sub> under reduced pressure. Propylene sulfide (PS; >98.0%, TCI), propylene oxide (*rac*-PO; >99.0%, TCI), and (*S*)-(-)-propylene oxide ((*S*)-PO; >98.0%, TCI) were purified by atmospheric distillation with CaH<sub>2</sub>

under argon flowing. 5-Norbornene-2,3-dicarboxylic anhydride (NA; >97.0%, TCI) was purified by sublimation before use. 1,4-Benzenedimethanol (BDM; >99.0%, TCI), trimethylolpropane (TMP; >98.0%, TCI), potassium pivalate (>98.0%, TCI), sodium trifluoroacetate (>98.0%, TCI), sodium acetate (>98.0%, TCI), sodium pivalate hydrate (>98.0%, TCI), lithium acetate (>98.0%, TCI), potassium acetate (>99.0%, Sigma–Aldrich), cesium acetate (>98.0%, TCI), and cesium pivalate (>97.0%, TCI) were dried under high vacuum at 100 °C for three days before use. Poly(ethylene glycol) monomethyl ether 400(PEG400; TCI), methyl acrylate (MA; >99.0%, TCI), and potassium thiocyanate (99.0%, Sigma–Aldrich) were used as received.

#### TYPICAL POLYMERIZATION PROCEDURES

**Polymerization of 2-ethylhexyl glycidyl ether (EHGE).** In the glovebox, EHGE (444 mg, 2.39 mmol), 1,4-benzenedimethanol (BDM) (6.00 mg, 43.5  $\mu$ mol), and cesium pivalate (5.09 mg, 21.7  $\mu$ mol) were mixed in a test tube. After sealing with a rubber septum, the test tube was taken out from the glovebox. The reaction was performed at 100 °C while stirring for 2.3 h and terminated by cooling down to room temperature. The product was purified via reprecipitation with methanol to produce poly(EHGE) as a colorless oil (253 mg). Yield: 57.0%. <sup>1</sup>H-NMR (400 MHz, CDCl<sub>3</sub>):  $\delta$  (ppm) 7.01-7.20 (m, 4H,  $-\text{C}_6\text{H}_4-$ ), 4.49 (s, 4H,  $-\text{C}_6\text{H}_4\text{CH}_2\text{O}-$ ), 3.39-3.75 (m, 5H  $\times$  n,  $-\text{OCH}_2\text{CHOCH}_2-$ ), 3.22-3.32 (m, 2H  $\times$  n,  $-\text{OCH}_2\text{CH}-$ ), 1.46 (t, 1H  $\times$  n,  $-\text{CH}_2\text{CH}(\text{CH}_2)_2$ ), 1.17-1.40 (m, 8H  $\times$  n,  $-\text{CH}_2\text{CH}(\text{CH}_2)\text{CH}_2\text{CH}_2\text{CH}_2\text{CH}_3$ ), 0.68-1.01 (m, 6H  $\times$  n,  $-\text{CH}_3$ ,  $-\text{CH}_3$ ).

**Polymerization of 2-(ethoxymethyl)thiirane (EMT).** In the glovebox, EMT (617 mg, 5.22 mmol), 2-phenylethanethiol (PET) (6.00 mg, 43.5  $\mu$ mol), and tributylphosphine (TBP) (44.0 mg, 217  $\mu$ mol) was dissolved in 0.6 mL THF solvent in a test tube. Cesium pivalate (3.05 mg, 13.0  $\mu$ mol) was subsequently added into this tube to start polymerization. The reaction was performed

at room temperature while stirring for 1 h and terminated by addition of 0.5 mL of methyl acrylate (MA). The product was purified via reprecipitation with methanol to give the poly(EMT) as a colorless stick liquid (322 mg). Yield: 52.2%.  $^1\text{H-NMR}$  (400 MHz, acetone- $d_6$ ):  $\delta$  (ppm) 7.22-7.33 (m, 5H,  $-\text{C}_6\text{H}_5$ ), 3.51-4.05 (m,  $4\text{H} \times n$ ,  $-\text{OCH}_2-$ ), 2.64-3.10 (m,  $3\text{H} \times n$ ,  $-\text{SCH}_2-$ ,  $-\text{SCHCH}_2-$ ), 1.02-1.37 (m,  $3\text{H} \times n$ ,  $-\text{CH}_3$ ).

## RESULTS AND DISCUSSION

### AMC-catalyzed ROP of epoxides

Initially, the ROP of EHGE was performed in the bulk at 100 °C under Ar using cesium pivalate (catalyst) and BDM (initiator) at a  $[\text{EHGE}]_0/[\text{BDM}]_0/[(\text{CH}_3)_3\text{CCOOCs}]$  molar ratio of 55/1.0/0.5. Polymerization was monitored by  $^1\text{H}$  NMR spectroscopy and was terminated when the EHGE conversion reached 75% (run 2 in Table 1). During polymerization, the dispersity ( $D_M$ ) of poly(EHGE) remained low (1.05–1.07), and the number-averaged molecular weight determined by NMR ( $M_{n,\text{NMR}}$ ) linearly increased with increasing EHGE conversion (Figure 1a), which indicated the controlled/living nature of the system. The  $^1\text{H}$  and  $^{13}\text{C}$  NMR spectra of poly(EHGE) (Figures S1 and S2) agreed with its expected structure, and  $M_{n,\text{NMR}}$  ( $8.0 \text{ kg mol}^{-1}$ ) was close to the theoretical value ( $M_{n,\text{th}}$ ) of  $7.6 \text{ kg mol}^{-1}$ . The size exclusion chromatography (SEC) trace of poly(EHGE) exhibited a single elution peak with a rather low  $D_M$  of 1.07 (Figure S3).

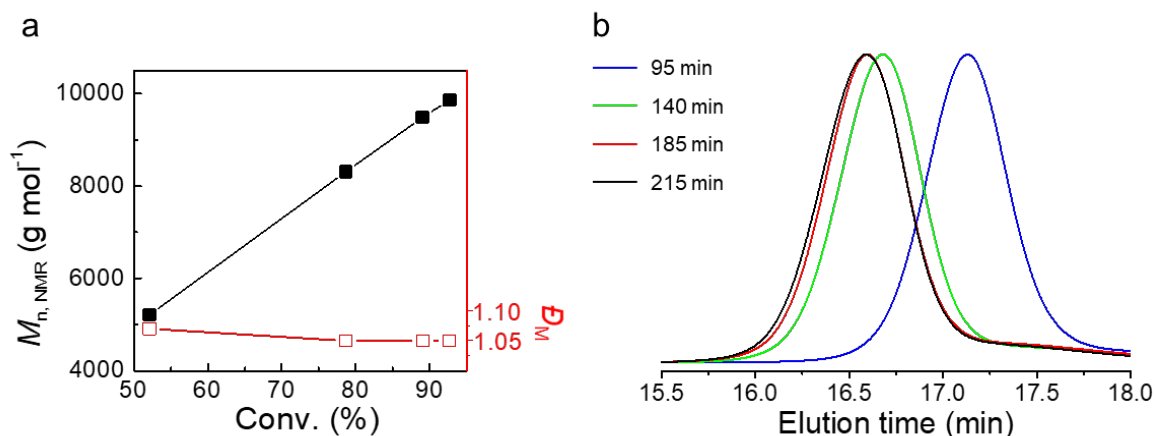


**Figure 1.** (a) Dependence of  $M_{n,NMR}$  (■) and  $D_M$  (□) on 2-ethylhexyl glycidyl ether conversion, (b) size exclusion chromatography traces of poly(2-ethylhexyl glycidyl ether) obtained at different polymerization times.

As AMC<sub>s</sub> can initiate the ROP of four-membered-ring lactones and oxetanes<sup>27,28</sup> as well as the ROAC of epoxides and cyclic anhydrides,<sup>26</sup> we examined the ability of cesium pivalate to initiate the ROP of epoxides and thus afford polyethers with pivalate  $\alpha$ -chain ends. The cesium pivalate-promoted ROP of EHGE proceeded in the absence of an alcohol initiator (run 6 in Table 1). Subsequent product analysis by Matrix-assisted laser desorption ionization time-of-flight mass spectrometry (MALDI-TOF MS) revealed the existence of a pivalate-initiated species (peak denoted by ▲ in Figure S4), a water-initiated species (peaks denoted by △ and ● in Figure S4), and a chain-transfer product (peak denoted by ○ in Figure S4). In contrast, the MALDI-TOF MS of poly(EHGE) synthesized using the cesium pivalate/BDM system demonstrated the absence of pivalate-initiated species (run 2 in Table 1 and Figure 2) and featured two series of peaks. The major series was assigned to BDM-initiated poly(EHGE) with the expected chemical structure, and the peak at  $m/z$  5563.81 was in line with the theoretical mass of the desired BDM-initiated

poly(EHGE) with a degree of 29 (calculated for  $[M + Na]^+ = 5563.71$ ). The minor series was assigned to water-initiated poly(EHGE) (calculated for  $[M + Na]^+ = 5628.87, n = 30$ ). Importantly, no signals attributable to carboxylate-initiated poly(EHGE) (calculated  $[M + Na]^+ = 5712.96, n = 30$ ) and chain-transfer products (calculated  $[M + Na]^+ = 5798.13, n = 30$ ) were observed. Hence, we concluded that in this catalyst/alcohol initiator system, rather than directly nucleophilically attack the activated epoxide to initiate its ring-opening, the carboxylate activated the initiator or the growing OH chain end via H-bonding to render the OH group sufficiently nucleophilic for attacking the monomer.

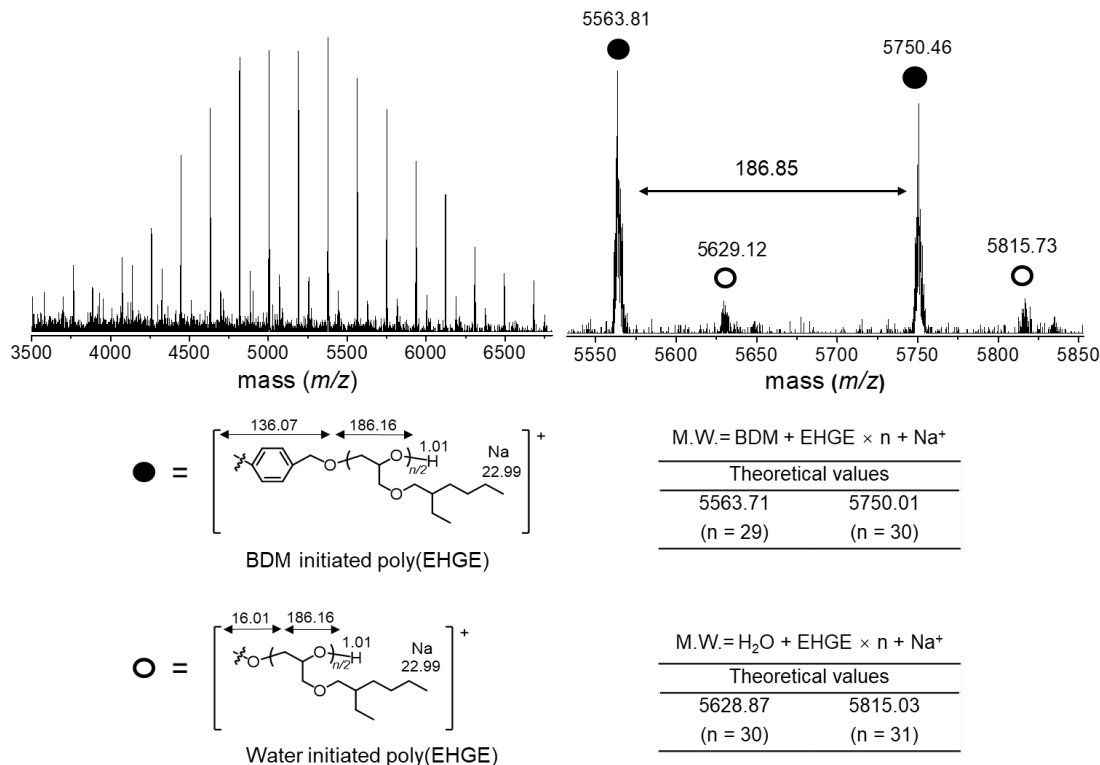


**Figure 2.** MALDI-TOF MS of poly(EHGE) synthesized in the presence of BDM initiator (polymerization was impeded in bulk under Ar atmosphere with the  $[\text{EHGE}]_0/[\text{BDM}]_0/[(\text{CH}_3)_3\text{CCOOCs}]$  ratio of 55/1.0/0.5 at 100°C, run2 in Table1).

The polymerization rate could be easily regulated by varying the catalyst loading (runs 4 and 5 in

Table 1), while the molecular weight distribution of the obtained polymer remained low ( $D_M = 1.07$  and  $1.11$ ). At the catalyst/initiator molar ratio of  $0.5/1.0$ ,  $M_{n,NMR}$  could be regulated in the range of  $5.0\text{--}20.0\text{ kg mol}^{-1}$  by adjusting the monomer/initiator ratio (runs 1–3 in Table 1). Chain extension experiments were executed to confirm the living nature of the system. Poly(EHGE) ( $M_{n,SEC} = 4.9\text{ kg mol}^{-1}$ ,  $D_M = 1.10$ ) was first prepared at an initial feed ratio of  $[\text{EHGE}]_0/[\text{BDM}]_0/[(\text{CH}_3)_3\text{CCOOCs}] = 55/1.0/0.5$ , and 55 equiv. of additional EHGE was introduced after complete monomer consumption. This addition immediately restarted chain propagation from the poly(EHGE) terminus to afford poly(EHGE) with a higher number-average molecular weight ( $M_{n,SEC} = 8.6\text{ kg mol}^{-1}$ ,  $D_M = 1.13$ ) (Figure S5), which confirmed that the present system enabled good control over polymerization and exhibited a controlled/living nature.

Our previous study indicated that AMCs with larger counteranions and stronger electron-donating groups on the carboxylate moiety show higher catalytic activity for the ROP of cyclic esters.<sup>23</sup> To confirm whether this was also the case for our epoxide ROP system, we examined the catalytic activities of pivalates, acetates, and trifluoroacetates with various counteranions ( $\text{Li}^+$ ,  $\text{Na}^+$ ,  $\text{K}^+$ , and  $\text{Cs}^+$ ; Figure 3). When AMCs with both  $\text{Li}^+$  and  $\text{Na}^+$  counteranions were tested for the ROP of EHGE, polymerization proceeded very slowly, e.g., in some cases, no polymerization was observed after 48 h. In contrast, AMCs with  $\text{K}^+$  and  $\text{Cs}^+$  counteranions effectively promoted the ROP of epoxides, and an increase in counteranion radius significantly enhanced the turnover frequency (TOF =  $2.9\text{ h}^{-1}$  for potassium pivalate vs.  $35.9\text{ h}^{-1}$  for cesium pivalate). This behavior was ascribed to the fact that with increasing radius of the counteranion, its association with the carboxylate anion becomes weaker, and carboxylate basicity increases. Thus, the carboxylate with a large counteranion radius is suitable in terms of catalytic activity. Meanwhile,  $\text{Cs}^+$  need to be carefully removed from the resulting products for medical applications because cytotoxicity of

cesium have been reported.<sup>29</sup> The comparison of cesium acetate with cesium pivalate revealed that stronger electron-donating groups on the alkyl moiety increase catalytic activity, i.e., the TOF (35.9 h<sup>-1</sup>) of cesium pivalate exceeded that of cesium acetate (5.43 h<sup>-1</sup>). This trend was also observed for potassium pivalate (TOF = 2.9 h<sup>-1</sup>) and potassium acetate (TOF = 0.0 h<sup>-1</sup>), in which case no catalytic activity was observed for potassium acetate in view of the relatively weak electron-donating nature of its substituents. The kinetic plots obtained for potassium pivalate-, cesium acetate-, and cesium pivalate-catalyzed ROP of EHGE exhibited first-order behavior (Figure S6) and revealed that catalytic activity followed the order of potassium pivalate < cesium acetate < cesium pivalate.

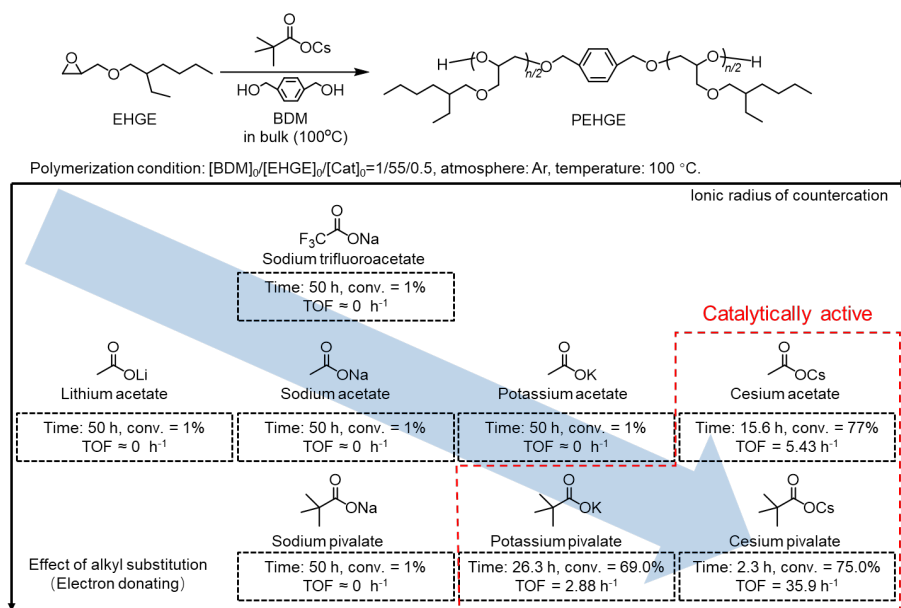


**Figure 3.** Catalytic performance of alkali metal carboxylates for the ring-opening polymerization of 2-ethylhexyl glycidyl ether.

**Table 1.** Results of cesium pivalate-catalyzed ring-opening polymerization of 2-ethylhexyl

glycidyl ether

Run	[EHGE] <sub>0</sub> /[BDM] <sub>0</sub> / [(CH <sub>3</sub> ) <sub>3</sub> COOCs]	Temp. (°C)	Conv. <sup>a</sup> (%)	Time (h)	<i>M</i> <sub>n,th</sub> <sup>b</sup> (g mol <sup>-1</sup> )	<i>M</i> <sub>n,NMR</sub> <sup>c</sup> (g mol <sup>-1</sup> )	<i>M</i> <sub>n,SEC</sub> <sup>d</sup> (g mol <sup>-1</sup> )	<i>D</i> <sub>M</sub> <sup>d</sup>
1	25/1.0/0.50	100	98	1.8	4,500	5,000	3,700	1.06
2	55/1.0/0.50	100	75	2.3	7,600	8,000	4,500	1.07
3	110/1.0/0.50	100	91	6.0	18,600	19,300	8,800	1.13
4	55/1.0/0.35	100	72	7.5	7,300	6,100	4,400	1.07
5	55/1.0/0.20	100	98	16	10,000	10,200	6,700	1.11
6	55/0.0/1.0	100	95	21	9,700	ND <sup>e</sup>	6,300	1.13

All polymerizations were performed with 43.5 μmol BDM and varied epoxides and catalyst loading in bulk.

<sup>a</sup>Calculated from <sup>1</sup>H NMR data. <sup>b</sup>*M*<sub>n,th</sub> = [M]<sub>0</sub>/[initiator]<sub>0</sub> × (conv.) × (M.W. of monomer) + (M.W. of initiator). <sup>c</sup>Determined by <sup>1</sup>H NMR analysis of the obtained polymer in CDCl<sub>3</sub>. <sup>d</sup>*M*<sub>n,SEC</sub> and *D*<sub>M</sub> were estimated by size exclusion chromatography using polystyrene calibration in tetrahydrofuran at 40 °C. <sup>e</sup>Not determined.

### Monomer scope and limitations

To investigate the monomer scope and limitations, we examined the cesium pivalate-catalyzed ROP of alkyl-substituted epoxides (1,2-epoxyhexane (EH), cyclohexene oxide (CHO), (1,2-butylene oxide) BO, and epichlorohydrin (ECH)), styrene oxide (SO), and glycidyl ethers (ethyl glycidyl ether (EGE), allyl glycidyl ether (AGE), and benzyl glycidyl ether (BGE)) (Scheme 1, Table 2). SO showed low reactivity and was fully consumed only after 48 h to afford poly(SO) with a relatively high *D*<sub>M</sub> of 1.41. A higher polymerization rate and better polymerization control were achieved in the case of EH, which was converted into well-defined poly(EH) with a monomodal molecular weight distribution (*D*<sub>M</sub> = 1.18). The highest reactivity and the best

molecular weight controllability ( $D_M = 1.05$ ) among the alkyl-substituted epoxides were obtained for BO, which featured short alkyl substituents. Besides, by applying a high monomer-to-initiator ratio, a high molecular weight poly(1,2-butylene oxide) (PBO) was obtained with a narrow  $D_M$  ( $M_{n,SEC} = 32 \text{ kg mol}^{-1}$ ,  $D_M = 1.29$ ; run 7 in Table 2). Compared to alkyl-substituted epoxides, glycidyl ethers exhibited higher polymerization rates. EGE possesses a structure similar to that of EHGE but exhibited higher ROP reactivity and afforded poly(EGE) with low dispersity ( $D_M = 1.07$ ). Even faster polymerization was observed for the ROP of BGE, and the related polymerization controllability remained high ( $D_M = 1.09$ ). To examine the feasibility of functional polyether synthesis, we tested a monomer with a double bond on the substituent (AGE), obtaining a well-defined functional polyether (poly(AGE),  $D_M = 1.12$ ). In a previously reported potassium alkoxide/naphthalenide-initiated AGE polymerization system, polymerization was often accompanied by the isomerization of the allyl repeating unit at temperatures above 40 °C.<sup>30, 31</sup> However, <sup>1</sup>H NMR analysis showed that in the present polymerization, the allyl group of AGE was not isomerized even at 100 °C (Figure 4), which indicated that our system allowed for post-polymerization modification. The polymerizations of CHO and ECH were unsuccessful. In the case of CHO, the initiator/propagating chain end may be less accessible to the sterically encumbered 1,2-disubstituted epoxide ring. In the case of ECH, a strong electron-withdrawing group on the  $\alpha$ -carbon decreases the electron density on the oxyanionic end of the growing chain, thus significantly reducing its ability to nucleophilically attack the monomer. Alternatively, the carboxylate can directly attack the chloromethylene group of ECH. The SEC traces and <sup>1</sup>H NMR spectra of the obtained polyethers are presented in Figures S7–S12. In the SEC traces of some of

the obtained polyethers, a shoulder peak in the high molecular region was observed, especially in the case of poly(EH). To investigate the origin of the shoulder peak, preparative SEC was employed to isolate the high-molecular-weight component of poly(EH), which was then subjected to MALDI-TOF MS analysis. As shown in Figure S13, the high-molecular-weight poly(EH) was confirmed to be a water-initiated polyether. From the kinetic analysis (Figure S6), an induction period was observed in the present polymerization system. Thus, given that water can initiate polymerization faster than the alcohol initiator (BDM), it can be considered that the water-initiated species grew first in the induction period and resulted in the high molecular weight shoulder.

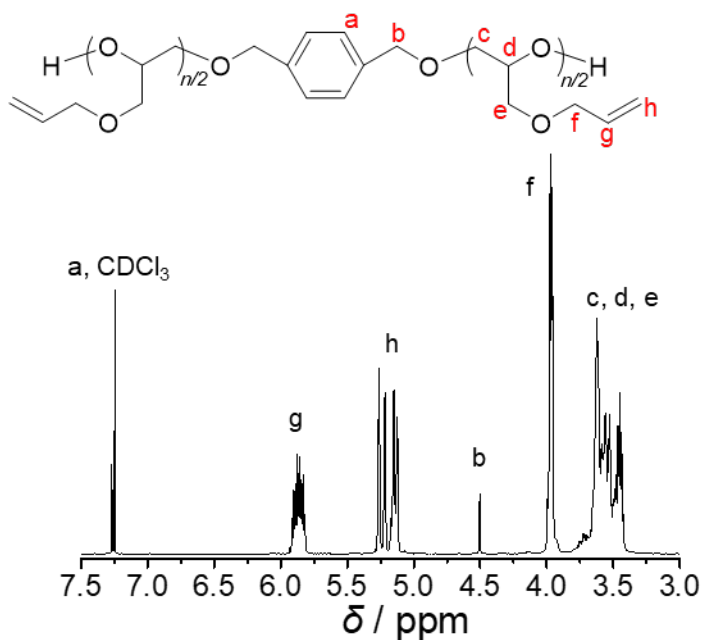


**Figure 4.** <sup>1</sup>H NMR spectrum of poly(AGE) (run 2 in Table 2).

The MALDI-TOF MS of the obtained products confirmed the expected BDM-initiated polyether structure and also revealed the presence of water-initiated species (Figures S14–S19). The water-

initiated species was ascribed to the contamination of monomers with small amounts of water or monomer-derived glycol, the removal of which is very difficult and typically requires multiple distillations.<sup>32,33</sup> Notably, the carboxylate-initiated polymerization and chain transfer were suppressed in the ROP of all monomers, as evidenced by the related MALDI-TOF MS.

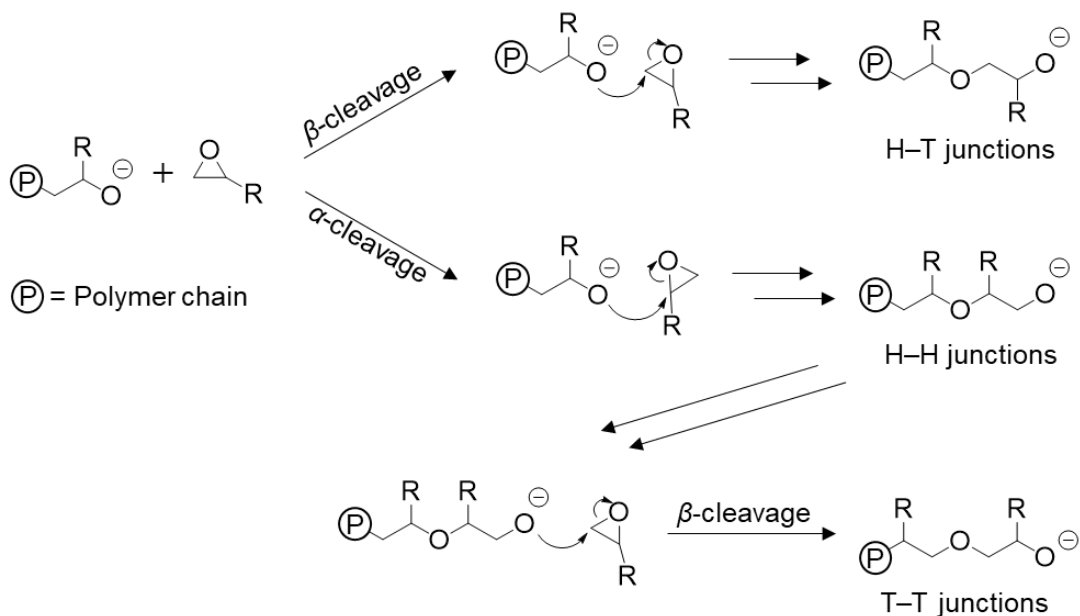
**Table 2.** Results of cesium pivalate–catalyzed ring-opening polymerization of various epoxides.

Run	Monomer	[M] <sub>0</sub> /[BDM] <sub>0</sub> /[(CH <sub>3</sub> ) <sub>3</sub> COOCs]	Conv. (%) <sup>a</sup>	Time (h)	<i>M</i> <sub>n,th</sub> <sup>b</sup>	<i>M</i> <sub>n,NMR</sub> <sup>c</sup>	<i>M</i> <sub>n,SEC</sub> <sup>d</sup>	<i>D</i> <sub>M</sub> <sup>d</sup>
1	EGE	55/1.0/0.5	80	1.6	4,500	6,000	4,500	1.07
2	AGE	55/1.0/0.5	93	3.0	5,800	6,400	4,100	1.12
3	BGE	55/1.0/0.5	89	1.3	8,000	ND <sup>f</sup>	4,300	1.09
4	SO	55/1.0/0.5	99	48	6,500	ND <sup>f</sup>	2,200	1.41
5	EH	55/1.0/0.5	80	13	4,400	3,000	2,600	1.18
6	BO	110/1.0/0.5	82	8.0	6,500	7,300	5,900	1.05
7	BO	1,400/1.0/1.0	96	48	96,900	ND <sup>e</sup>	31,900	1.29
8	CHO	55/1.0/0.5	-	-	-	-	-	-
9	ECH	55/1.0/0.5	-	-	-	-	-	-
10	<i>rac</i> -PO	107/1.0/0.5	ND <sup>e</sup>	7.0	ND <sup>e</sup>	5,500	4,600	1.07
11	( <i>S</i> )-PO	107/1.0/0.5	ND <sup>e</sup>	11	ND <sup>e</sup>	4,800	4,200	1.06

All polymerizations were performed with 43.5 μmol BDM with varied epoxides and catalyst loading at 100 °C in bulk. <sup>a</sup>Calculated from <sup>1</sup>H NMR data. <sup>b</sup> $M_{n,th} = [M]_0/[initiator]_0 \times (conv.) \times (M.W. \text{ of monomer}) + (M.W. \text{ of initiator})$ . <sup>c</sup>Determined by <sup>1</sup>H NMR analysis of the obtained polymer in CDCl<sub>3</sub>. <sup>d</sup>*M*<sub>n,SEC</sub> and *D*<sub>M</sub> were estimated by size exclusion chromatography using polystyrene calibration in tetrahydrofuran at 40 °C. <sup>e</sup>Not determined because of the evaporation of PO during polymerization. <sup>f</sup>Not determined, as the <sup>1</sup>H NMR signals of the initiator residue overlapped with the signals from polymer main chain or was too small.

To study the selectivity of the nucleophilic attack ( $\alpha$ - or  $\beta$ -cleavage) during AMC-catalyzed ROP, we heated an equimolar mixture of methanol and PO in the presence of cesium pivalate at 100 °C for 12 h. <sup>1</sup>H, <sup>13</sup>C, heteronuclear multiple quantum correlation (HMQC), and quantitative <sup>13</sup>C NMR (Figures S20, S21) analyses showed that the  $\alpha$ - to  $\beta$ -cleavage ratio equaled 6.5:93.5, i.e., the epoxide ring-opening mainly occurred through the nucleophilic attack of the initiator at the  $\beta$ -carbon, and subsequent propagation followed the  $\beta$ -cleavage pathway shown in Scheme 2. This

regioselectivity was in line with a previous report.<sup>13</sup>



**Scheme 2.** Chain propagation mechanism.

### Stereoregular polyether synthesis

To explore the possibility of stereoregular polyether synthesis, we applied our catalyst system to the ROP of an optically pure epoxide monomer. Initially, we carried out the cesium pivalate-catalyzed ROP of racemic PO (*rac*-PO) at a  $[\text{PO}]_0/[\text{BDM}]_0/[(\text{CH}_3)_3\text{COOCs}]$  molar ratio of 107/1.0/0.5. The obtained poly(propylene oxide) (PPO) showed the predicted  $M_{n,\text{NMR}}$  ( $5.5 \text{ kg mol}^{-1}$ ) and a low  $D_M$  (1.07, run 10 in Table 2). The corresponding  $^{13}\text{C}$  NMR spectrum (Figure 5) featured four peaks in the range of 75.1–75.7 ppm (denoted as a'), which originated from the *mm*, *rr*, and *rm/rm* triads of the main-chain methine group (*mm*: 26%, *rr*: 25%, *rm/rm*: 49%). Peaks corresponding to the *m* and *r* dyad structure of the main-chain methylene group (*m*: 52%, *r*: 48%)

were observed at 72.8–73.6 ppm (denoted as b'). The highly split carbon signals corresponding to the methine (a') and methylene (b') groups in the polymer main chain demonstrated the atactic configuration of the synthesized PPO.<sup>18,34,35</sup> These results implied that the AMC-catalyzed ROP of racemic epoxides was neither iso- nor syndiospecific. Next, the ROP of optically pure (*S*)-propylene oxide ((*S*)-PO) (*ee* > 98%) was performed under the same condition (run 11 in Table 2). The  $M_{n,NMR}$  of the obtained isotactic-enriched PPO (*iso*-PPO) was close to that of PPO, and polymerization proceeded in a well-controlled manner ( $\mathcal{D}_M = 1.06$ ). The <sup>13</sup>C NMR spectrum of *iso*-PPO exhibited sharp peaks at 73.5 and 75.6 ppm (Figure 5) due to the *mm* triad of the methine group (*mm*: 89.3%, *rr*: 3.9%, *rm/mr*: 6.8%) and the *m* diad of the methylene group in the main chain (*m*: 93.9%, *r*: 6.1%), respectively, which strongly suggested an isotactic structure. The formation of small amounts of *rr* and *rm/mr* triads for the main-chain methine group was caused by the racemization of (*S*)-PO during polymerization.<sup>36</sup> This was confirmed by the optical purity decrease of (*S*)-PO upon reacting with cesium pivalate at 100 °C for 3 h (Figure S22). To further prove the isotacticity of the obtained polymer, we examined its crystallization behavior by differential scanning calorimetry (DSC). As shown in Figure S23, peaks due to the melting and crystallization of *iso*-PPO were observed, corroborating the isotactic configuration. The glass transition temperature ( $T_g$ ) of *iso*-PPO equaled –67.2 °C and was close to that reported for highly isotactic PPO<sup>34</sup> ( $T_g = -66.8$  °C for isotactic PPO with *mm* triad > 99% and  $M_{n,SEC} = 13.7$  kg mol<sup>-1</sup>). On the other hand, the melting temperature ( $T_m = 48.5$  °C) was lower than the literature value ( $T_m = 62.9$  °C), which could be due to the lower molecular weight and *mm* content of our polymer. Thus, we confirmed the suitability of our system for the synthesis of crystallizable isotactic-

enriched polyethers, which are of interest as novel photodegradable polymers.<sup>37</sup>

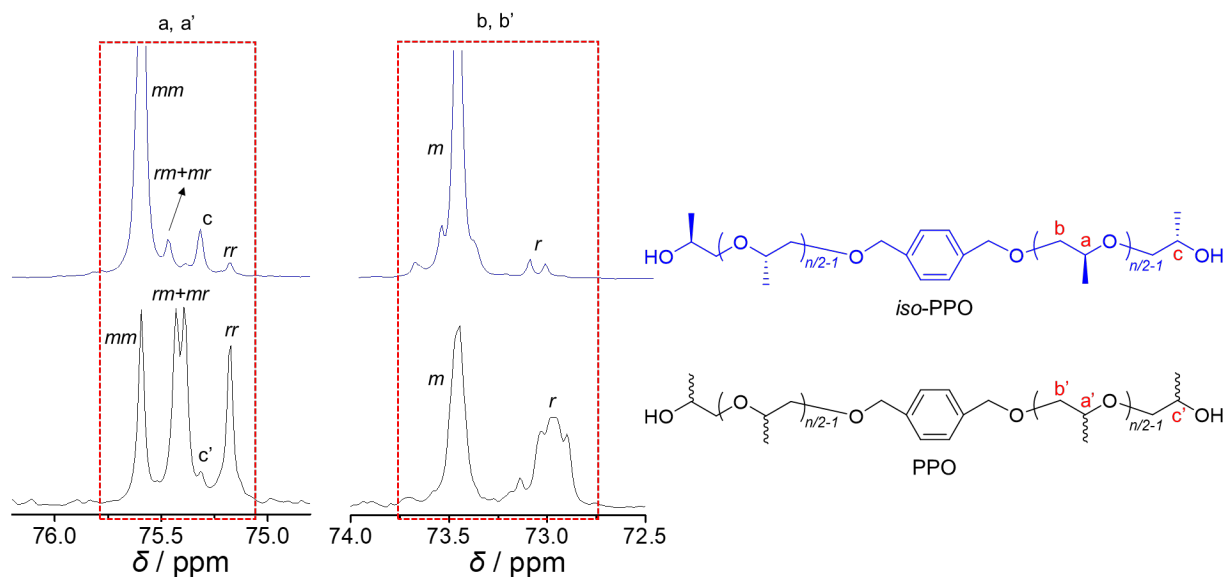


**Figure 5.**  $^{13}\text{C}$  nuclear magnetic resonance spectra of isotactic-enriched (blue) and atactic (black) PPO.

### ROP of EHGE with different initiators

**Table 3.** Synthesis of poly(2-ethylhexyl glycidyl ether) in the presence of different initiators.

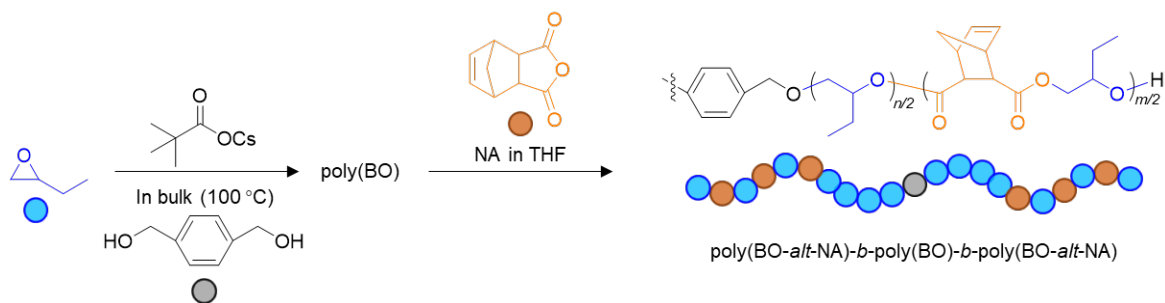
Run	Initiator	$[\text{EHGE}]_0/[\text{initiator}]_0$ $/[(\text{CH}_3)_3\text{COOCs}]$	Conv. (%) <sup>a</sup>	Time (h)	$M_{n,\text{th}}$ <sup>b</sup>	$M_{n,\text{NMR}}$ <sup>c</sup>	$M_{n,\text{SEC}}$ <sup>d</sup>	$D_M^d$
1	PPA	55/1.0/0.5	95.0	4.3	9,700	9,700	5,200	1.16
2	TMP	55/1.0/0.5	87.5	3.6	8,900	10,700	5,000	1.09
3	MDA	55/1.0/0.5	89.3	2.8	9,100	10,800	6,300	1.07
4	PEG 400	55/1.0/0.5	98.0	4.6	10,400	10,900	6,300	1.20

All polymerizations were performed with 43.5  $\mu\text{mol}$  initiator with EHGE (444 mg, 2.39 mmol) and cesium pivalate (5.09 mg, 21.7  $\mu\text{mol}$ ) at 100  $^\circ\text{C}$  in bulk. <sup>a</sup>Calculated from  $^1\text{H}$  NMR data. <sup>b</sup> $M_{n,\text{th}} = [\text{M}]_0/[\text{initiator}]_0 \times (\text{conv.}) \times (\text{M.W. of monomer}) + (\text{M.W. of initiator})$ . <sup>c</sup>Determined by  $^1\text{H}$  NMR analysis of the obtained

polymer in  $\text{CDCl}_3$ .  $^dM_{n, \text{SEC}}$  and  $D_M$  were estimated by size exclusion chromatography using polystyrene calibration in tetrahydrofuran at 40 °C.

To further demonstrate the utility of our polymerization system, we used various functional initiators to prepare polyethers with different chain ends (Scheme 1; Figures S24–S27). When 3-phenyl-1-propanol (PPA) was used to initiate the ROP of EHGE with cesium pivalate, polymerization proceeded smoothly, and the obtained polymer showed a low  $D_M$  (run 1 in Table 3). The ROP of EHGE initiated by trimethylolpropane (TMP) afforded three-armed star-shaped poly(EHGE) (run 2 in Table 3) with a well-defined structure ( $D_M = 1.09$ ), which implied that chain growth uniformly proceeded from each initiating site. A well-defined cationizable polyether was also prepared using *N*-methyldiethanolamine (MDA) as an amino-functionalized initiator (run 3 in Table 3). Such cationizable polymers are widely employed for gene delivery.<sup>38,39,40</sup> Besides, poly(ethylene glycol) monomethyl ether (PEG400;  $M_n = 400 \text{ g mol}^{-1}$ ) was used as a macroinitiator to prepare a block copolyether in one step. The polymerization could be well controlled, as evidenced by the relatively low dispersity of the obtained product ( $D_M = 1.20$ , run 4 in Table 3). These results proved that our ROP system is well suited for the synthesis of end-functionalized polyethers and block copolyethers.

### One-pot synthesis of polyether-polyester block copolymer



**Scheme 3.** One-pot synthesis of polyether-polyester block copolymer.

Inspired by the ability of AMCs to efficiently promote the ROAC of cyclic anhydrides and epoxides,<sup>24,25</sup> we employed our system to achieve the one-pot synthesis of a polyether-polyester block copolymer using the second feeding of a cyclic anhydride into the epoxide polymerization mixture (Scheme 3). A PBO diol was prepared using cesium pivalate as the catalyst and BDM as the initiator at a  $[\text{BO}]_0/[\text{BDM}]_0/[(\text{CH}_3)_3\text{CCOOCs}]$  molar ratio of 160/1/0.5 at 100 °C. When the BO conversion reached 36.3%, 40 equivalents (with respect to BDM) of 5-norbornene-2,3-dicarboxylic anhydride (NA) was added to start the ROAC of BO and NA. The product obtained at a NA consumption of 44.6% exhibited a SEC elution peak in a higher-molecular-weight region (Figure 6) compared to that observed for PBO diol, and <sup>1</sup>H NMR analysis confirmed the chemical structure of each block (Figure S28). The integral intensity of the signal assigned to the alkenyl protons on the norbornene ring (i) was two times that of the signal assigned to the methine group (k) of the epoxide of the poly(BO-*alt*-NA) block, which implied that during ROAC, NA and BO were consumed in equal amounts. In addition, the DOSY NMR spectrum of the obtained block copolymer showed only one diffusion coefficient (except for the solvent signal), which confirmed that the two blocks were covalently linked (Figure S29). These results indicated the successful synthesis of a poly(BO-*alt*-NA)-*b*-PBO-*b*-poly(BO-*alt*-NA) triblock copolymer via the formation of PBO diol and the subsequent bidirectional growth of poly(BO-*alt*-NA). The low  $D_M$  (1.05) of this copolymer suggested good molecular weight controllability. The DSC analysis of poly(BO-*alt*-NA)-*b*-PBO-*b*-poly(BO-*alt*-NA) (Figure S30) revealed two  $T_g$  values ( $T_{g, \text{PBOblock}} \approx -65$  °C;<sup>41</sup>  $T_{g, \text{poly(BO-}i\text{alt-NA)block}} \approx 54$  °C) that originated from PBO and poly(BO-*alt*-NA) blocks and were comparable to those of the corresponding homopolymers ( $T_{g, \text{PBO}} \approx -73$  °C; <sup>41</sup>  $T_{g, \text{poly(BO-}i\text{alt-NA)}} \approx 53$  °C, Figure S31). This finding implies that the PBO and poly(BO-*alt*-NA) blocks were microphase-separated and suggests that the corresponding copolymer can be used as a

thermoplastic elastomer.

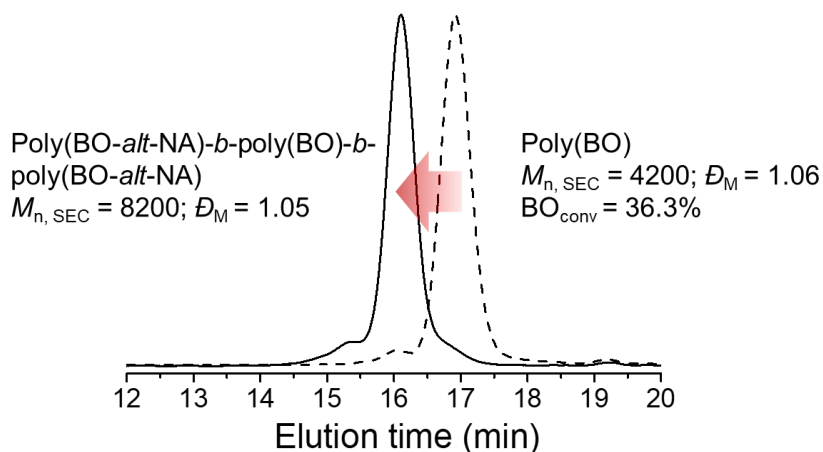


**Figure 6.** Size exclusion chromatography traces of poly(butylene oxide) diol (dotted line) and poly(butylene oxide *-alt-5-norbornene-2,3-dicarboxylic anhydride*)-*b*-poly(butylene oxide)-*b*-poly(butylene oxide *-alt-5-norbornene-2,3-dicarboxylic anhydride*) (solid line).

### AMC-catalyzed ROP of episulfides

**Table 4.** Cesium pivalate–catalyzed ring-opening polymerization of episulfides.

Run	Monomer	$[M]_0/[PET]_0/[(CH_3)_3COOCs]/[TBP]$	Conv. (%) <sup>a</sup>	Time (h)	$M_{n,th}$ <sup>b</sup>	$M_{n,NMR}$ <sup>c</sup>	$M_{n,SEC}$ <sup>d</sup>	$D_M$ <sup>d</sup>
1	EMT	120/1.0/0.3/5.0	96.0	1.0	13,600	13,800	10,600	1.17
2	EHOMT	120/1.0/0.3/5.0	>99	1.0	24,200	ND <sup>e</sup>	16,800	1.15
3	PS	120/1.0/0.3/5.0	>99	1.0	8,900	8,700	2,600	1.35
4	BT	120/1.0/0.3/5.0	>99	1.0	13,900	ND <sup>e</sup>	11,200	1.06

Polymerizations were performed at room temperature with 0.6 mL tetrahydrofuran as solvent. PET (6.00 mg, 43.5  $\mu$ mol), TBP (44.0 mg, 217  $\mu$ mol), cesium pivalate (3.05 mg, 13.0  $\mu$ mol), and 5.22 mmol monomer were used in polymerization. <sup>a</sup>Calculated from <sup>1</sup>H NMR data. <sup>b</sup> $M_{n,th} = [M]_0/[initiator]_0 \times (conv.) \times (M.W. \text{ of monomer}) + (M.W. \text{ of initiator})$ . <sup>c</sup>Determined by <sup>1</sup>H NMR analysis of the obtained polymer in CDCl<sub>3</sub>. <sup>d</sup> $M_n$ ,

$M_{SEC}$  and  $D_M$  were estimated by size exclusion chromatography using polystyrene calibration in tetrahydrofuran at 40 °C. °Not determined, as the  $^1\text{H}$  NMR signals of the initiator residue overlapped with those of the polymer main chain.

Compared to polyethers, polythioethers exhibit higher backbone flexibility, as the C–S bond is longer and weaker than the C–O bond.<sup>42</sup> Besides, the high oxidative reactivity and hydrophobicity of polythioethers make them promising hydrophobic segments for oxidation-responsive nanocontainers.<sup>43,44</sup> Hence, we examined the ability of AMCs to promote the ROP of episulfides. Different kinds of episulfides were synthesized in accordance with reported method,<sup>45</sup> and the products were characterized by  $^1\text{H}$  and  $^{13}\text{C}$  NMR spectra (Figures S32–S37). The ROP of 2-(ethoxymethyl)thiirane (EMT) was carried out with PET as the initiator and cesium pivalate as the catalyst at room temperature. TBP was added as the reducing agent to minimize the unwanted formation of disulfide bonds.<sup>46</sup> Since episulfides are highly reactive, the polymerization in the bulk is uncontrollable. Thus, tetrahydrofuran (THF) was employed as the solvent to control the reaction, though the resulted polythioether still exhibited higher dispersity than polyether.

. MA was added to quench the polymerization and end-cap the polymer chain end. Molecular weight linearly increased with increasing monomer conversion (Figure S38), and the corresponding kinetic plot showed first-order behavior (Figure S39). The polymerization was complete in 1 h, affording poly(EMT) with a low  $D_M$  (run 1 in Table 4). This behavior demonstrated that the employed AMC showed high catalytic efficiency for episulfide ROP and allowed for effective molecular weight control. However, even in the presence of excess reducing agent, we observed disulfide formation, i.e., thiolates from two chain-ends were connected to form

the polymer chains with an internal disulfide bond, which gave rise to a small SEC peak with a molecular weight two times that of the desired product (Figure S40). Using MALDI-TOF MS, we confirmed the existence of poly(EMT) with the 2-phenylethane-1-thiolate/methyl propionate chain end together with a small amount of poly(EMT) with an internal disulfide bond and 2-phenylethane-1-thiolate chain ends (Figure S41). Besides, our system efficiently promoted the ROP of other substituted episulfides such as propylene sulfide (PS), butylthiirane (BT), and 2-(((2-ethylhexyl)oxy)methyl)thiirane (EHOMT) (Table 4, Figure S42), i.e., featured a broad substrate scope.

### **Catalytic mechanism**

Finally, we investigated the mechanism of AMC-catalyzed ROP by performing Fourier transform infrared (FT-IR) spectroscopy measurements to elucidate the interaction between the initiator and AMC as well as that between the monomer and AMC. In view of its liquid nature and ease of handling, PPA was used as the alcohol initiator to investigate the interaction between cesium pivalate and hydroxyl groups. The peak at  $\sim 3417\text{ cm}^{-1}$  due to the stretching vibration of the hydroxyl group in the FT-IR spectrum of PPA slightly shifted to lower frequencies upon mixing with cesium pivalate (Figure 7a)<sup>23</sup> because of the H-bonding-induced decrease in the O–H bond order.<sup>47,48</sup> This behavior implied that cesium pivalate can activate the hydroxyl groups of the propagating chain ends/initiators. Furthermore, the peak corresponding to the symmetric C–O vibration of EHGE shifted to higher frequencies in the presence of cesium pivalate (Figure 7b),<sup>26,49</sup> which indicated that the cesium cation weakened the C–O bond and activated the epoxide ring.<sup>50</sup> Therefore, we concluded that the AMC-catalyzed ROP of epoxides features a dual activation mechanism in which the alkali metal cation and carboxylate activate the epoxide and the hydroxyl

group on the initiator and propagating chain end, respectively. According to the reported mechanism of the base-mediated anionic ROP of episulfides,<sup>51,52</sup> it is reasonable to conclude that cesium pivalate could also activate the thiol groups on the propagating chain ends/initiators as well as the episulfide monomer in the same way as in the alcohol/epoxide system. Here, the activation mechanism may involve both mono- and bimetallic pathways (Figure 7c). Importantly, the activation behavior of the monomer and initiator/propagating chain end would be finely controlled by adjusting the counteranion and carboxylate moiety, which is one of the strong advantages of our AMC catalyst system.

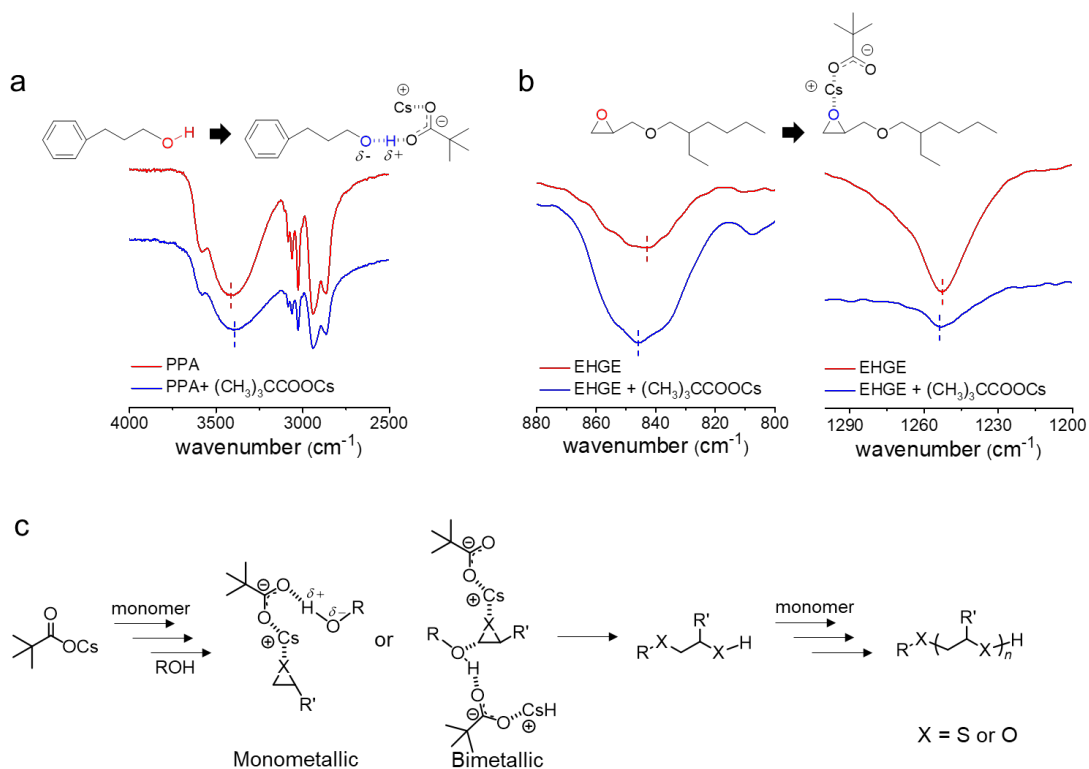


**Figure 7.** (a) FT-IR of (a) 3-phenyl-1-propanol (red) and 3-phenyl-1-propanol + cesium pivalate (blue) recorded at 100 °C and (b) 2-ethylhexyl glycidyl ether (red) and 2-ethylhexyl glycidyl ether + cesium pivalate (blue) recorded at 100 °C. (c) Proposed catalytic mechanism.

## CONCLUSION

This study demonstrated that AMCs can be used as simple and efficient catalysts for the ROP of epoxides and episulfides to obtain polyethers and polythioethers with predictable molecular weights and low dispersity. Compared to the traditional alkali metal alkoxide-mediated epoxide ROP system, the AMC system offers the benefits of excellent molecular weight controllability and a broad substrate and initiator (alcohol) scope. The absence of direct initiation by carboxylate anions in the presence of an alcohol initiator provided an opportunity to precisely synthesize functional polyethers such as end-functionalized homopolymers, block copolyethers, and topologically unique polyethers using various functional alcohol initiators. Moreover, in the presence of a reducing agent, the AMC system could be applied to the ROP of diverse episulfides to produce well-defined polythioethers. Thus, the above advantages of AMCs, together with their low cost and ease of handling, make them well suited for both laboratory- and industrial-scale polyether/polythioether production.

## ASSOCIATED CONTENT

**Supporting Information.** The Supporting Information is available free of charge at

XXXXXXXXXXXXXXXXXXXX

NMR spectra, SEC traces, DSC trace, and MALDI-TOF spectra of synthesized polymers, kinetic

plot of EHGE with different AMC-catalysts, dependence of  $M_n$ , NMR on the monomer conversion for cesium pivalate-catalyzed EMT ROP, and kinetic plot for the EMT ROP (file type, i.e., PDF)

## AUTHOR INFORMATION

### Corresponding Author

\***Takuya Isono** – *Division of Applied Chemistry, Faculty of Engineering, Hokkaido University, Sapporo 060-8628, Japan; orcid.org/0000-0003-3746-2084; Email: isono.t@eng.hokudai.ac.jp*

\***Toshifumi Satoh** – *Division of Applied Chemistry, Faculty of Engineering, Hokkaido University, Sapporo 060-8628, Japan; orcid.org/0000-0001-5449-9642; Email: satoh@eng.hokudai.ac.jp*

### Author Contributions

‡T.-L. G and ‡X.-C. X. These authors contributed equally.

### Notes

The authors declare no conflict of interest.

## ACKNOWLEDGMENTS

This work was financially supported by the Japan Society for the Promotion of Science Grant-in-Aid for Scientific Research (B) (Grant No. 19H02769), the Ministry of Education, Culture, Sports, Science, and Technology of Japan Grant-in-Aid for Scientific Research on Innovative Areas (Hybrid Catalysis for Enabling Molecular Synthesis on Demand; Grant Nos. 18H04639 and 20H04798), the Frontier Chemistry Center (Hokkaido University), the Photo-Excitonic Project

(Hokkaido University), the Creative Research Institution (CRIS, Hokkaido University), the Project of Junior Scientist Promotion (Hokkaido University), the Inamori Foundation, and the Hokkaido University DX Doctoral Fellowship (Grant No. JPMJSP2119).

## ABBREVIATIONS

Ring-opening polymerization, ROP; propylene oxide, PO; ring-opening alternating copolymerization, ROAC; alkali metal carboxylate, AMC; 2-ethylhexyl glycidyl ether, EHGE; 1,4-benzenedimethanol, BDM; nuclear magnetic resonance, NMR; size exclusion chromatography, SEC; matrix-assisted laser desorption ionization time-of-flight mass spectrometry, MALDI-TOF MS; turnover frequency, TOF; 1,2-epoxyhexane, EH; cyclohexene oxide, CHO; 1,2-butylene oxide, BO; epichlorohydrin, ECH; styrene oxide, SO; ethyl glycidyl ether, EGE; allyl glycidyl ether, AGE; benzyl glycidyl ether, BGE; 3-phenyl-1-propanol, PPA; trimethylolpropane, TMP; *N*-methyldiethanolamine, MDA; 5-norbornene-2,3-dicarboxylic anhydride, NA; 2-(ethoxymethyl)thiirane, EMT; 2-phenylethanethiol, PET; tributylphosphine, TBP; methyl acrylate, MA; Fourier transform infrared, FT-IR.

## REFERENCES

- (1) Kang, T.; Banquy, X.; Heo, J.; Lim, C.; Lynd, N. A.; Lundberg, P.; Oh, D. X.; Lee, H. K.; Hong, Y. K.; Hwang, D. S.; Waite, J. H.; Israelachvili, J. N.; Hawker, C. J. Mussel-Inspired Anchoring of Polymer Loops That Provide Superior Surface Lubrication and Antifouling Properties. *ACS Nano* **2016**, *10*(1), 930–937.
- (2) Paderes, M. C.; James, C.; Jamieson, S. A.; Mai, A. H.; Limon, J. H.; Dolatkhani, M.; Fernandez-Prieto, S.; De Borggraeve, W. M.; Fratini, E. Tuning the Properties of Polyether

- Alkyl Urea Derivatives as Rheology Modifiers in Cosmetic Solvents. *ACS Appl. Polym. Mater.* **2020**, *2*(7), 2902–2909.
- (3) Obermeier, B.; Wurm, F.; Mangold, C.; Frey, H. Multifunctional Poly(Ethylene Glycol)S. *Angew. Chemie - Int. Ed.* **2011**, *50*(35), 7988–7997.
- (4) Kim, M.; Park, J.; Lee, K. M.; Shin, E.; Park, S.; Lee, J.; Lim, C.; Kwak, S. K.; Lee, D. W.; Kim, B.-S. Peptidomimetic Wet-Adhesive PEGtides with Synergistic and Multimodal Hydrogen Bonding. *J. Am. Chem. Soc.* **2022**, *144*(14), 6261–6269.
- (5) Son, I.; Lee, Y.; Baek, J.; Park, M.; Han, D.; Min, S. K.; Lee, D.; Kim, B. S. PH-Responsive Amphiphilic Polyether Micelles with Superior Stability for Smart Drug Delivery. *Biomacromolecules* **2021**, *22* (5), 2043–2056.
- (6) Hill, F. B.; Young, C. A.; Nelson, J. A.; Arnold, R. G. Glycol, P. Urethane Rubber from a Polyether Glycol Properties of Raw Polymer and Vulcanizates-Properties of Raw Polymer and Vulcanizates. *Industrial & Engineering Chemistry* **1956**, *48*(5), 927–929.
- (7) Johnson, G. H.; Mancl, L. A.; Schwedhelm, E. R.; Verhoef, D. R.; Lepe, X. Clinical Trial Investigating Success Rates for Polyether and Vinyl Polysiloxane Impressions Made with Full-Arch and Dual-Arch Plastic Trays. *J. Prosthet. Dent.* **2010**, *103*(1), 13–22.
- (8) Veronese, F. M.; Pasut, G. M10. PEGylation, Successful Approach. *Drug Discov. Today* **2005**, *10*(21), 1451–1458.
- (9) Price, C. C. Polyethers. *Accounts of Chemical Research* **1974**, *3538*(2), 294–301.
- (10) Penczek, S.; Cypryk, M.; Duda, A.; Kubisa, P.; Słomkowski, S. Living Ring-Opening Polymerizations of Heterocyclic Monomers. *Prog. Polym. Sci.* **2007**, *32*(2), 247–282.

- (11) Ding, J.; Heatley, F.; Price, C.; Booth, C. Use of Crown Ether in the Anionic Molecular Weight and Molecular Weight Distribution. *European polymer journal* **1991**, *27*(9), 895–899.
- (12) Stolarzewicz, A.; Neugebauer, D.; Grobelny, Z. Influence of the Crown Ether Concentration and the Addition of Tert-butyl Alcohol on Anionic Polymerization of (Butoxymethyl)Oxirane Initiated by Potassium Tert-butoxide. *Macromol. Chem. Phys.* **1995**, *196* (4), 1295–1300.
- (13) Billouard, C.; Desbois, P.; Deffieux, A. “Controlled” High-Speed Anionic Polymerization of Propylene Oxide Initiated by Alkali Metal Alkoxide/Trialkylaluminum Systems. *Macromolecules* **2004**, *37*(11), 4038–4043.
- (14) Gervais, M.; Labbé, A.; Carlotti, S.; Deffieux, A. Direct Synthesis of  $\alpha$ -Azido, $\omega$ -Hydroxypolyethers by Monomer-Activated Anionic Polymerization. *Macromolecules* **2009**, *42*(7), 2395–2400.
- (15) Billouard, C.; Desbois, P.; Deffieux, A.; Berland, P.; Cedex, P.; Ag, B.; Ludwigshafen, D.-; February, R. V; Re, V.; Recci, M.; May, V. Controlled High-Speed Anionic Polymerization of Propylene Oxide Initiated by Onium Salts in the Presence of Triisobutylaluminum. *Macromolecules* **2007**, *40*(22) 7842–7847.
- (16) Carlotti, S.; Labbé, A.; Rejsek, V.; Doutaz, S.; Gervais, M.; Deffieux, A. Living/Controlled Anionic Polymerization and Copolymerization of Epichlorohydrin with Tetraoctylammonium Bromide-Triisobutylaluminum Initiating Systems. *Macromolecules* **2008**, *41*(19), 7058–7062.

- (17) Lipinski, B. M.; Walker, K. L.; Clayman, N. E.; Morris, L. S.; Jugovic, T. M. E.; Roessler, A. G.; Getzler, Y. D. Y. L.; MacMillan, S. N.; Zare, R. N.; Zimmerman, P. M.; Waymouth, R. M.; Coates, G. W. Mechanistic Study of Isotactic Poly(Propylene Oxide) Synthesis Using a Tethered Bimetallic Chromium Salen Catalyst. *ACS Catal.* **2020**, *10*(15), 8960–8967.
- (18) Peretti, K. L.; Ajiro, H.; Cohen, C. T.; Lobkovsky, E. B.; Coates, G. W. A Highly Active, Isospecific Cobalt Catalyst for Propylene Oxide Polymerization. *J. Am. Chem. Soc.* **2005**, *127*(33), 11566–11567.
- (19) Kaminsky, W.; Funck, A.; Hähnsen, H. New Application for Metallocene Catalysts in Olefin Polymerization. *Dalt. Trans.* **2009**, *41*, 8803–8810.
- (20) Jones, W. D. Diverse Chemical Applications of N-Heterocyclic Carbenes. *J. Am. Chem. Soc.* **2009**, *131*(42), 15075–15077.
- (21) Raynaud, J.; Absalon, C.; Gnanou, Y.; Taton, D. Polymerization of Ethylene Oxide and Direct Synthesis of *r*,  $\omega$ -Difunctionalized Poly(Ethylene Oxide)s and Poly(Ethylene Oxide)-*b*-Poly( $\epsilon$ -Caprolactone) Block Copolymers. *J. Am. Chem. Soc.* **2009**, *131*(6), 3201–3209.
- (22) Xia, Y.; Shen, J.; Alamri, H.; Hadjichristidis, N.; Zhao, J.; Wang, Y.; Zhang, G. Revealing the Cytotoxicity of Residues of Phosphazene Catalysts Used for the Synthesis of Poly(Ethylene Oxide). *Biomacromolecules* **2017**, *18*(10), 3233–3237.
- (23) Saito, T.; Aizawa, Y.; Yamamoto, T.; Tajima, K.; Isono, T.; Satoh, T. Alkali Metal Carboxylate as an Efficient and Simple Catalyst for Ring-Opening Polymerization of Cyclic

- Esters. *Macromolecules* **2018**, *51*(3), 689–696.
- (24) Xia, X.; Suzuki, R.; Gao, T.; Isono, T.; Satoh, T. One-Step Synthesis of Sequence-Controlled Multiblock Polymers with up to 11 Segments from Monomer Mixture. *Nature Communications* **2022**, *13*, 163
- (25) Xia, X.; Suzuki, R.; Takojima, K.; Jiang, D. H.; Isono, T.; Satoh, T. Smart Access to Sequentially and Architecturally Controlled Block Polymers via a Simple Catalytic Polymerization System. *ACS Catal.* **2021**, *11*(10), 5999–6009.
- (26) Chen, C. M.; Xu, X.; Ji, H. Y.; Wang, B.; Pan, L.; Luo, Y.; Li, Y. S. Alkali Metal Carboxylates: Simple and Versatile Initiators for Ring-Opening Alternating Copolymerization of Cyclic Anhydrides/Epoxides. *Macromolecules* **2021**, *54*(2), 713–724.
- (27) Koinuma, H., Naito, K.; Hirai, H. Anionic polymerization of oxiranes and cyclic siloxanes initiated with potassium salt-crown ether systems. *Die Makromolekulare Chemie* **1982**, *183*(6) 1383-1392.
- (28) Juzwa, M.; Jedlin, Z. Novel Synthesis of Poly(3-Hydroxybutyrate). *Macromolecules* **2006**, *39*(13), 4627–4630.
- (29) Ghosh, A.; Sharma, A.; Talukder, G. Effects of Cesium on Cellular Systems. *Biol. Trace Elem. Res.* **1993**, *38*(2), 165–203.
- (30) Lee, B. F.; Kade, M. J.; Chute, J. A.; Gupta, N.; Campos, L. M.; Fredrickson, G. H.; Kramer, E. J.; Lynd, N. A.; Hawker, C. J. Poly(Allyl Glycidyl Ether)-A Versatile and Functional Polyether Platform. *J. Polym. Sci. Part A Polym. Chem.* **2011**, *49*(20), 4498–4504.
- (31) Obermeier, B.; Frey, H. Poly (Ethylene Glycol-co-Allyl Glycidyl Ether) S : A PEG-Based

- Modular Synthetic Platform for Multiple Bioconjugation. *Bioconjugate Chemistry* **2011**, 22(3), 436-444.
- (32) Ryzhakov, D.; Printz, G.; Jacques, B.; Messaoudi, S.; Dumas, F.; Dagorne, S.; Le Bideau, F. Organo-Catalyzed/Initiated Ring Opening Co-Polymerization of Cyclic Anhydrides and Epoxides: An Emerging Story. *Polym. Chem.* **2021**, 12(20), 2932–2946.
- (33) Driscoll, O. J.; Stewart, J. A.; McKeown, P.; Jones, M. D. Ring-Opening Copolymerization Using Simple Fe(III) Complexes and Metal- and Halide-Free Organic Catalysts. *Macromolecules* **2021**, 54(18), 8443–8452.
- (34) Ghosh, S.; Lund, H.; Jiao, H.; Mejía, E. Rediscovering the Isospecific Ring-Opening Polymerization of Racemic Propylene Oxide with Dibutylmagnesium. *Macromolecules* **2017**, 50(3), 1245–1250.
- (35) Herzberger, J.; Niederer, K.; Pohlit, H.; Seiwert, J.; Worm, M.; Wurm, F. R.; Frey, H. Polymerization of Ethylene Oxide, Propylene Oxide, and Other Alkylene Oxides: Synthesis, Novel Polymer Architectures, and Bioconjugation. *Chemical reviews* **2016**. 116(4), 2170–2243.
- (36) Childers, M. I.; Longo, J. M.; Van Zee, N. J.; Lapointe, A. M.; Coates, G. W. Stereoselective Epoxide Polymerization and Copolymerization. *Chem. Rev.* **2014**, 114(16), 8129–8152.
- (37) Lipinski, B. M.; Morris, L. S.; Silberstein, M. N.; Coates, G. W. Isotactic Poly(Propylene Oxide): A Photodegradable Polymer with Strain Hardening Properties. *J. Am. Chem. Soc.* **2020**, 142(14), 6800–6806.
- (38) Van Bruggen, C.; Hexum, J. K.; Tan, Z.; Dalal, R. J.; Reineke, T. M. Nonviral Gene

- Delivery with Cationic Glycopolymers. *Acc. Chem. Res.* **2019**, *52*(5), 1347–1358.
- (39) Abd Elwakil, M. M.; Gao, T.; Isono, T.; Sato, Y.; Elewa, Y. H. A.; Satoh, T.; Harashima, H. Engineered  $\epsilon$ -Decalactone Lipomers Bypass the Liver to Selectively: In Vivo Deliver mRNA to the Lungs without Targeting Ligands. *Mater. Horizons* **2021**, *8*(8), 2251–2259.
- (40) Miller, J. B.; Zhang, S.; Kos, P.; Xiong, H.; Zhou, K.; Perelman, S. S.; Zhu, H.; Siegwart, D. J. Non-Viral CRISPR/Cas Gene Editing In Vitro and In Vivo Enabled by Synthetic Nanoparticle Co-Delivery of Cas9 mRNA and SgRNA. *Angew. Chemie* **2017**, *129*(4), 1079–1083.
- (41) Lai, J.; Trick, G. S. Glass Transformation Temperatures of Polymers of Olefin Oxides and Olefin Sulfides. *J Polym Sci Part A-1 Polym Chem.* **1970**, *8*(9), 2339–2350.
- (42) He, C.; Zhang, C.; Zhang, O. Synthesis and Thermal Properties of Polythioether-Based Liquid-Crystalline Polymers Containing Azobenzene in the Side Chain. *Polym. Int.* **2009**, *58*(9), 1071–1077.
- (43) Napoli, A.; Valentini, M.; Tirelli, N.; Müller, M.; Hubbell, J. A. Oxidation-Responsive Polymeric Vesicles. *Nat. Mater.* **2004**, *3*(3), 183–189.
- (44) Rehor, A.; Schmoekel, H.; Tirelli, N.; Hubbell, J. A. Functionalization of Polysulfide Nanoparticles and Their Performance as Circulating Carriers. *Biomaterials* **2008**, *29*(12), 1958–1966.
- (45) Gorjizadeh, M.; Afshari, M. A Facile and Convenient Method for Synthesis of Thiiranes under Mild Condition Using Phase Transfer Catalyst. *Orient. J. Chem.* **2013**, *29*(4), 1657–1660.

- (46) Matsumura, S.; Hlil, A. R.; Lepiller, C.; Gaudet, J.; Guay, D.; Shi, Z.; Holdcroft, S.; Hay, A. S. Stability and Utility of Pyridyl Disulfide Functionality in RAFT and Conventional Radical Polymerizations. *J. Polym. Sci. Part A Polym. Chem.* **2008**, *46*(21), 7207–7224.
- (47) Chakarova, K.; Hadjiivanov, K. H-Bonding of Zeolite Hydroxyls with Weak Bases: FTIR Study of CO and N<sub>2</sub> Adsorption on H-D-ZSM-5. *J. Phys. Chem. C* **2011**, *115*(11), 4806–4817.
- (48) Makarova, M. A.; Ojo, A. F.; Karim, K.; Hunger, M.; Dwyer, J. FTIR Study of Weak Hydrogen-Bonding of Bronsted Hydroxyls in Zeolites and Aluminophosphates. *J. Phys. Chem.* **1994**, *98*(14), 3619–3623.
- (49) Gontrani, L.; Nunziante Cesaro, S.; Stranges, S.; Bencivenni, L.; Pieretti, A. FTIR Spectra and Density Functional Theory P.E.D. Assignments of Oxiranes in Ar Matrix at 12 K. *Spectrochim. Acta-Part A Mol. Biomol. Spectrosc.* **2014**, *120*, 558–567.
- (50) Vigasin, A. A.; Schriver-Mazzuoli, L.; Schriver, A. Systematic Trends in the Vibrational Frequency Shifts of Some Molecules Trapped in Amorphous Water Ice. *J. Mol. Struct.* **2003**, *658*(1–2), 101–113.
- (51) Napoli, A.; Tirelli, N.; Kilcher, G.; Hubbell, J. A. New Synthetic Methodologies for Amphiphilic Multiblock Copolymers of Ethylene Glycol and Propylene Sulfide. *Macromolecules* **2001**, *34*(26), 8913–8917.
- (52) Kuhlmann, M.; Singh, S.; Groll, J. Controlled Ring-Opening Polymerization of Substituted Episulfides for Side-Chain Functional Polysulfide-Based Amphiphiles. *Macromolecular rapid communications* **2012**, *33*(17), 1482–1486.